International Journal on
"Technical and Physical Problems of Engineering"
(IJTPE)
Published by International Organization of IOTPE

ISSN 2077-3528
IJTPE Journal
www.iotpe.com
ijtpe@iotpe.com

September 2024 | Issue 60 | Volume 16 | Number 3 | Pages 251-257

FORMULATION AND STRUCTURAL ANALYSIS OF IRON OXIDE-BASED POWDER COMPOSITES AND THEIR PROPERTIES

C.A. Aliev [1] J.V. Asgarov [2] A.M. Guliyeva [2]

1. Azerbaijan Technical University, Baku, Azerbaijan, ilham85@inbox.ru
2. Azerbaijan University of Architecture and Construction, Baku, Azerbaijan
c.askerov@mail.ru, azizaquliyeva1960@gmail.com

Abstract- The article presents the theoretical and technological foundations for determining the formulations of compositions consisting of metal powders, iron, its oxides and carbon. It has been established that when obtaining blanks of complex shape, the amount of carbon and carbon-containing resin should take into account the rheological properties of the composition. In this case, ultrafine particles (0.2-0.4 μ_m) of iron oxide were used, and the powder mixtures were refined by cold pressing at a pressure of 400 MPa. A packing model for compaction of ultrafine Fe_2O_3 particles and iron powder using a polymer binder is constructed. Experimental data on the compacted mixture were obtained depending on the fractional composition of the powders. The following are the results of studies of compositions "iron-oxide binding" obtained by cold pressing the following components: iron powder Pj_2M_3, particles of oxide Fe_2O_3, phenol-formaldehyde resin. After that, the compositions were subjected to additional operations. To achieve a high density of compacts, three technological options were carried out: sintering, hot pressing and hot upsetting. It was found that the compaction of compacts in these operations is complex and depends on the proportion of oxide in the composition of the compositions.

Keywords: Formulation, Rheological Properties, Iron-Oxide-Binding, Structure, Properties, Composition, Sintering, Pressing, Shrinkage, Sediment, Oxide Phase, Hydroge.

1. INTRODUCTION

From literary sources [1-3] it follows that the compositions "metals-oxides-binding" are used for the purpose of:

- Manufacturing of shaped blanks obtained directly by compression pressing and subsequent sintering, as well as for casting methods (MIM - process). As a binder in these compositions, a carbon-containing resin is used;
- Production of blanks and semi-finished products obtained from granules after reaction grinding, subsequent compaction and pressure treatment.

Both options provide for the reduction of oxides inside the solid phase with highly dispersed carbon. In view of this, for each of the above options when choosing (determining) the formulation of the compositions, there are different approaches.

The production of these compositions of the "iron-oxide-binding " type by cold pressing of these components followed by sintering or hot pressing and settling of antifriction parts, for example, O-rings, is a serious scientific and technical problem. So, for example, a rational choice of the proportion of each constituent composition is required, taking into account the dispersion of their particles. In addition, it is of interest to study the contribution of cold pressing of composites and additional operations of compacting compacts to the structure and properties of the material. The presence of iron oxide and a carbon-containing binder in the charge of iron-based compositions can intensify the processes of reduction, compaction and hardening of workpieces during heating operations. In other words, the presence of oxide can lead to activated sintering of the composition.

Therefore, the study of oxide-carbon-containing powder compositions is also interesting from the point of view of obtaining workpieces of high density and strength by sintering. Taking into account the publications [4-9] devoted to the issue under study, in planning and conducting research, it was supposed to study the influence of specific factors of the developed technology on the above processes. These include the high dispersion of the components of the compositions, associated with the high dispersion of primary materials or the high dispersion of the phases that form during reaction grinding, as well as the structure of materials obtained as a result of low-temperature firing of the compositions.

2. EXPERIMENTAL TECHNIQUE

The rational composition of the composition consisted of the following components, wt.%: Iron oxide Fe_2O_3 with a particle size of 0.2-0.4 μ_m-42; reduced iron powder PJ 2M3, resin SFJ3031-15.2 and zinc stearate 0.18%. The charge of the composition was cold pressed under a pressure of 400 MPa. In order to obtain high-density compacts, three technological options were used: sintering, compression hot pressing and hot upsetting.

Registered: 240310 Article Info: 1861 Accepted: 240816
Reserved: 240603 Available: 240930

Sintering was studied on compositions used to study the processes of binder degradation and low-temperature heat treatment, as well as on compositions to study the effect of various factors on sintering. In the compositions, the ratio between the amount of iron powder and waste, the dispersion of their components, as well as the degree of filling of their components, as well as the degree of filling them with a solid phase (y_i and y_2) changed.

Samples with an outer diameter of 30 mm, an inner diameter of 15 mm and a height of 5 mm and blanks with dimensions of 20×20×80 mm were made from the investigated compositions. Dimensions, density, hardness were measured on round specimens, structure was determined, and mechanical properties on rectangular specimens. The samples were heated without air access for the destruction of the binder, after which they were heated for three hours in a vacuum environment at a temperature of 8000C. Next, the samples were subjected to high-temperature sintering in a hydrogen or endogas environment. Then the dimensions, density, mechanical properties were measured and the structure was studied.

The tensile strength and elongation were determined on the samples according to UOCT 1497-84, and structural studies using the methods of X-ray diffraction, scanning and transmission electron microscopy, metallography. The discussion of the results. For MIM technology in composites (MIM feedstocks), the ratio between the solid phase and the binder is chosen from the point of view of formability. The volume fraction of the binder should be such that the composition is fluidized during molding. At the same time, the ratio of the mass fractions of the binder and oxides should ensure the preservation of the carbon balance, taking into account the carbon formed as a result of the destruction of the resin.

When choosing the formulation of the compositions, the main influencing factor is that in any composition the solid phase consists of sharply different substances, metal powders and their oxides. From the point of view of rheological properties, these compositions are not fully understood. The production of a large number of formulations of metal- oxide-resin compositions and the experimental determination of their characteristics is very labor-intensive. Therefore, in order to determine the rheological properties of compositions, including viscosity, it is necessary to develop a model - a method for calculating them.

These composition models allow us to understand the physical processes occurring during molding, as well as to identify ways to optimize their compositions and properties. When developing models, the following are used:

- Newton's equation, representing the relationship between the force of friction and viscosity;
- Movement in the composition is laminar;
- Irrotational flow fields are composed by simple superposition;
- Deformation of the composition is carried out by mutual displacement of rubbing surfaces. Particles of the solid phase in the composition are evenly distributed.

Let us first turn our attention to compositions consisting of a one-component solid phase. We take the following notation:

M is the total mass of fillers in units of volume;
m is the mass of one particle;
D is the diameter of the filler particle
r is the radius of the filler particle;
p is density of the particle of the filler material;
N is the number of filler particles in volumetric units;
N_s is the number of particles per sliding area;
S is the sliding surface area;
F_s is the friction force on the sliding area S;
a is distance between the areas connecting the centers of particles falling on adjacent areas moving towards each other;
Δ is the distance between the closest particles of adjacer
t is slip areas;
γ is the volume fraction of the composition occupied by the filler;
V_1 is the speed of movement of the i-th sliding surface;
η is dynamic viscosity of the binder;
h_k is dynamic viscosity of the composition.

3. BUILDING A TASK MODEL

For simplicity, let's turn to the simplest model. To construct it, we will make assumptions.

a) Solid round particles with the same radius are used as filler;
b) Packing of filler particles looks like a simple cube;
c) Material flow is ensured by simple interchange of densely packed surfaces.

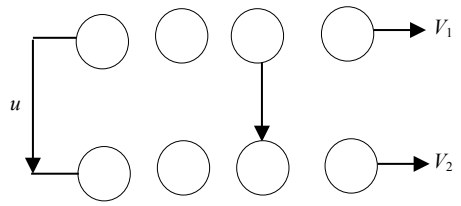

Figure 1. Stationary state between surfaces moving at different speeds (V_1 and V_2)

The number of filler particles in volumetric units will be:

$$N_v = \frac{M}{m} = \frac{3M}{4\pi r^3 \rho}, \text{ since } M = \frac{4}{3}\pi r^3 \rho$$

Likewise, $N_1 = (N_v)^{\frac{2}{3}} = (\frac{3M}{4\pi r^3 \rho})^{\frac{2}{3}}$

In a steady state between the surfaces moving at different speeds (V_1 and V_2) as Figure 1, the friction force FS appears. This force is determined only by the viscosity of the binder and the distance between sliding surfaces [4].

$$F_3 = S \times h \frac{V_1 - V_2}{a - 2r} \quad (1)$$

where, $a = (\frac{3M}{4\pi r^3 \rho})^{\frac{1}{3}}$.

After certain transformations and replacements, we get:

$$F_1 = \frac{1}{1-2r(\frac{3M}{4\pi r^2\rho})^{\frac{2}{3}}} \times \eta \times S \times \frac{V_1 - V_2}{a} \quad (2)$$

where, I_1 is seen that in Equation (2) the factor in front $S \times \frac{V_1 - V_2}{a}$ of the value is the effective viscosity of the composition (η_k).

Making substitutions and calculations, we get:

$$\frac{\eta_k}{\eta} = \frac{1}{1-1\times 242a^{\frac{1}{3}}}$$

where, $a = \frac{M}{\rho}$.

The considered simple model will give very high values of viscosity, because layers and particles have the ability to change their location in more free spaces. This increases the thickness of the thin layers involved in sliding. In the case under consideration, the velocities V_1 and V_2 are directed perpendicular to the layer surface. In the refined model in Figure 2, it is assumed that the particles in the rubbing surfaces are located at the tops of the squares, and the panicles in the section perpendicular to the sliding direction are located at the vertices of the triangles (hexagonal packing; in this case, the distance between the particles both in the sliding surfaces and in the perpendicular surfaces are always the same).

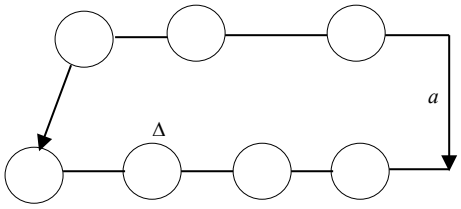

Figure 2. Updated model

At this time, the sliding surface area increases and becomes equal to $S = \frac{1}{\cos 30°}$. In a unit of volume, the number of particles will be:

$$N_v = \frac{M}{m} = \frac{1}{(D+\Delta)^3 \times \cos 30^\circ} \quad (4)$$

$$m = \frac{\pi D^3}{6}\rho \quad (5)$$

$$F_3 = \frac{S}{\cos 30°} \times \eta \times \frac{V_1 - V_2}{\Delta} \quad (6)$$

Solving together Equations (4) and (5), it is possible to determine the value of Δ:

$$\Delta = D[(\frac{\pi\rho}{6M\cos 30°})^{\frac{1}{3}} - 1] \quad (7)$$

Substituting Equation (7) into Equation (6) and taking into account that:

$$a = (D+\Delta)\cos 30° = (\frac{\pi\rho}{6M\cos 30°})^{\frac{1}{3}} D\cos 30°$$

we get

$$F_S = S\eta \times \frac{V_1 - V_2}{a} \times \frac{1}{1-(\frac{6M\cos 30°}{\pi\rho})^{\frac{1}{3}}} = \quad (8)$$

$$= S\eta \times \frac{V_1 - V_2}{a} \times \frac{1}{1-1.182\gamma^{\frac{1}{3}}}$$

In the steady state, the expression for the viscosity of the composition will take the form:

$$\eta_k = \frac{\eta}{1-1.182\gamma^{\frac{1}{3}}} \quad (9)$$

At the beginning of deformation, immediately after the application of (3) pressure, while the flow regime is uncertain and therefore additional friction will be involved (F_{S_2}). This force is determined by the movement of the filler particles relative to the binder, and its maximum value can be determined using Stokes' law [4]:

$$F_{S2} = \frac{1}{2}3\pi\eta SD(\frac{6M}{\pi D^3\rho})^{\frac{2}{3}} \times (V_1 - V_2) =$$

$$= \frac{2}{3}\pi(\frac{6M}{\pi\rho})^{\frac{1}{3}} \times \frac{\cos 30°}{\sqrt[3]{\cos 30°}} \times \eta S \frac{V_1 - V_2}{a}$$

As noted above, the factor before $S\frac{V_1 - V_2}{a}$ determines the effective viscosity of the composition. After calculations, this viscosity will be equal to:

$$\eta_{k2} = 5.31\gamma^{\frac{1}{3}}$$

At the beginning of deformation, the expression for the viscosity of a one-component composition takes the form:

$$\eta_{k2} = (5.31\gamma^{\frac{1}{3}} + \frac{1}{1-1.182\gamma^{\frac{1}{3}}})\eta \quad (11)$$

Table 1. Change in design ratios $1\frac{\eta_k}{\eta}$ at different values γ

γ	0	0.005	0.01	0.05	0.1	0.2
$5.31\gamma^{\frac{1}{3}}$	0	0.9	1.17	1.96	2.5	3.13
$\frac{1}{1-1.182\gamma^{\frac{1}{3}}}$	1	1.25	1.35	1.79	2.22	3.33
$5.31\times a^{\frac{1}{3}} + \frac{1}{1-1.18a^{\frac{1}{3}}}$	1	2.15	2.52	3.75	4.72	6.46

0.4	0.45	0.5	0.55	0.6	0.605
3.93	4.04	4.22	4.35	4.49	0
7.94	10.0	16.67	33.33	826.4	∞
11.87	14.04	20.89	37.68	830.9	∞

From Table 1, it can be seen that during deformation in a transient mode, the viscosity oi the deformed composition, depending on the value of γ, has three distinct regions: initial, when γ changes from 0 to 0.01, the viscosity increases 2.5 times; average, when, when γ changes from 0.01 to 0.4, i.e. 40 times, the viscosity of the composition monotonically increases 5 times; final, when, when γ changes from 0.45 to 0.605 by 1.5 times, the viscosity increases infinitely.

Table 1 also shows that up to γ=0.4, the viscosity is greatly influenced by the component reflecting the energy spent on the flow around the particles of the solid phase; at γ=0.4, the viscosity component due to the movement of particles plays a significantly greater role. An increase in shear is associated with a decrease in the distance between the sliding surfaces. It can be assumed that the viscosity value calculated by this model will be slightly higher than the measured one. This is due to the deviation of composition from Newton's composition. This is also due to the fact that real powders are able to disperse depending on the particle size. Small particles can be located between large particles, which increases the thickness of the binder layers between sliding surfaces [11-13]. In the case when the shape of the filler particles significantly differs from the spherical, the measured value of the viscosity may exceed the calculated one. For $\gamma = 0.605$ expression (9) tends to infinity. At this value of γ, the filling of the solid phase in MIM - feedstocks reaches its maximum value (~0.6) [11-19].

Apparently, expression (9) can be written as follows:

$$\eta_k = \frac{\eta}{1-\left(\frac{\gamma}{0.605}\right)^{\frac{1}{3}}} \tag{12}$$

where, 0.605 is the critical volume fraction of the solid phase at which the composition loses its fluidity (η=∞). This expression is valid only for the model under consideration. It can be assumed that, in general, at a steady state, the viscosity of a deformable composition can be expressed in the form;

$$\frac{\eta_k}{\eta} = \frac{A}{1-\left(\frac{\gamma}{\gamma_k}\right)^{\frac{1}{3}}} \tag{13}$$

where, A is the coefficient for various types of solid phases, determined as a result to experiments; die value of γ_k is also determined experimentally. At γ=0 Equation (13) loses its physical meaning. For MIM-feedstock of steel powder 3167, given in [13], depending on the value of γ, we use Equation (13) to display the experimental curve. For die case under consideration, the value γ=0.72 was determined experimentally.

To calculate the value of A on die experimental curve, select a point with coordinates $\eta_k / \eta = 10$ and $\gamma = 0.6$. Substituting them into Equation (13). we obtain the value $a = 0.59$. For the relative viscosity, the expression takes die form:

$$\frac{\eta_k}{\eta} = \frac{0.59}{1-\left(\frac{\gamma}{0.72}\right)^{\frac{1}{3}}} \tag{14}$$

The experimental and calculated values $\frac{\eta_k}{\eta}$ of the ratio versus γ are presented in Table 2.

Table 2. Experimental and calculated values $\frac{\eta_k}{\eta}$ of the ratio depending on the value of γ

The value of γ	0.1	0.2	0.3	0.4	0.5	0.6	0.65
Calculated value $\frac{\eta_k}{\eta}$	1.22	1.7	2.3	3.2	5.1	10.0	17.7
Experimental value $\frac{\eta_k}{\eta}$	1.36	1.6	2.2	3.2	5.0	10.0	16.5

Note: the experimental values were determined according to the graph given in [13].

It should be noted that such a high filling ($a = 0.72$) was obtained by a special choice of the particle size distribution of the powder [13]. From the data presented in Table 2, it can be concluded that when the content of the solid phase is within 0.1-0.65, the values of the viscosities obtained as a result of experiments and calculated according to the proposed model differ by no more than 10%.

Figure 3 shows the dependence of the viscosity "iron-oxide-binder" on the mass fraction of iron powder. The figure shows that with an increase in the content of iron powder, the viscosity of the "iron-oxide-binder" mass increases monotonically.

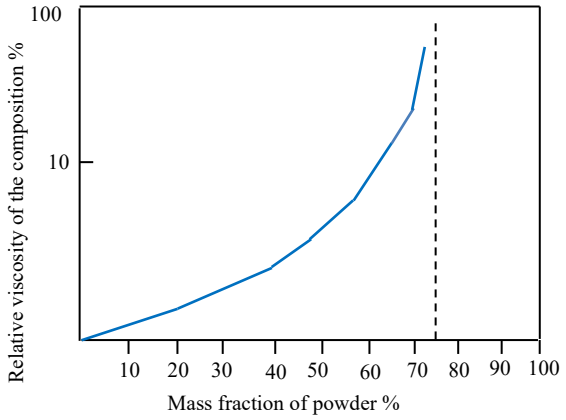

Figure 3. Dependence of the relative viscosity depending on the volume content of iron powder in a polyethylene bond

The results of experiments on cold pressing are shown in Figure 2. The abscissa shows the ratio of the mass of the oxide to the sum of the masses of the oxide and the metal phase in the initial compositions, multiplied by 100%, and the ordinate is the ratio of the actual density of the sample to the theoretical density of the sample to the theoretical density of carbon steel. Figure 3 shows that the amount of oxide significantly affects the relative density of the

sintered material. From Figure 4 that the dependence of compaction during sintering on the composition of the compositions is complex. With an increase in the proportion of oxide from 0 to 11%, the relative density does not change, and with a further increase in the proportion of oxide, it decreases. This is especially noticeable at relatively low temperatures of isothermal holding (1050-1150 °C).

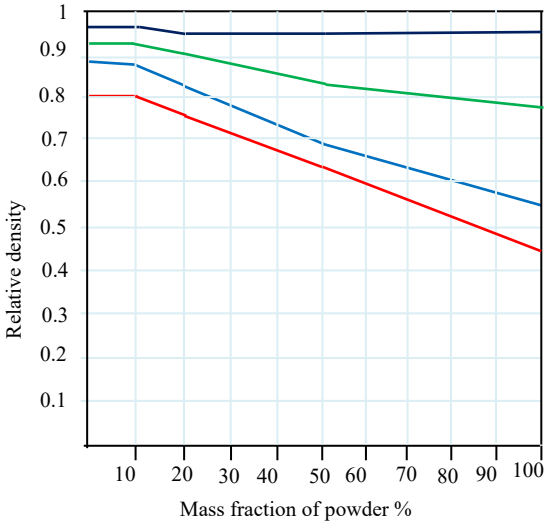

Figure 4. Influence of the fraction of the oxide phase in the solid component of the initial compositions on the relative density of materials sintered in hydrogen at sintering temperatures: 1) 1050 °C; 2) 1150 °C; 3) 1250 °C; 4)1350 °C

The structure of the compositions sintered in this temperature range is spongy iron, tine pores of which are not visible even at a magnification of 500 times. After etching with a 5% solution of nitric acid and at a magnification of 1000 times, pores with a size of 1...10 mkm are detected on a scanning probe microscope, however, the grain boundaries are not visible. No pores were found in the structure of the material sintered at 1300 °S. Etching in a solution of nitric and picric acids does not reveal grain boundaries. Gray spots in reflected electrons indicate the presence of an oxidized film on the surface. The grain boundaries are not revealed.

It can be assumed that the space between the iron particles is supplemented with spongy iron. Based on this, it is possible to calculate the volumetric shrinkage at various values of γ_1 and γ_2.

The iron content in 1 cm^3 of the compact will be:

$$m_{\max} = 7.8\times\gamma_1 + 5.24(1-\gamma_1)\gamma_2 \times 0.7 \quad (15)$$

where, γ_1 is the volumetric content of iron in the composition; γ_2 is the volumetric content of oxide in the binder.

The composition consisted, % of the mass: Fe_2O_3 oxide with particle sizes; 0, 2-0, 4 mkm-42; atomized iron powder, grade Pj2M3-15.2; zinc stearate-0.8.

During the destruction of the binder and sintering, there is a total change in volume by the value of ΔV, then the volume of 1 cm^3 of the compact will be $1-\Delta V$.

4. ANALYSIS OF THE RESULTS

The density of the sample after oxide reduction and sintering will be [20]:

$$\rho = \frac{7.8\gamma_1 + 5.24(1-\gamma_1)\times\gamma_2 0.7}{1-\Delta V} \quad (16)$$

The density of the spongy iron formed from oxides in the interparticle space will be:

$$\rho_{s.g.} = \frac{5.24(1-\gamma_1)\times\gamma_2 0.7}{1-\Delta V-\gamma_1} \quad (17)$$

The conditions for complete sintering $\left(\rho = \rho_{s.g.}\right)$ can be written as:

$$\Delta V = (1-\gamma_1)\times(1-0.47\gamma_2) \quad (18)$$

The results of calculating the values of ΔV are shown in Table 3.

Table 3. Theoretical values for volumetric shrinkage for uniform density

γ_2 \ γ_1	0.1	0.2	0.3	0.4	0.5	0.6
0,1	0.86	0.815	0.77	0.73	0.69	0.65
0.2	0.76	0.72	0.69	0.65	0.61	0.57
0.3	0.67	0.63	0.60	0.57	0.53	0.50
0.4	0.57	0.54	0.515	0.49	0.46	0.43
0.5	0.48	0.45	0.43	0.405	0.38	0.36
0.6	0.38	0.36	0.34	0.325	0.305	0.29

Based on Table 3, it can be assumed that for different γ_1/γ_2, the sintering mechanism may be different. For large γ_2/γ_1 i.e. With a high content of oxide, the kinetics of sintering is controlled by the sintering mechanism of sponge iron, and with a low compaction during sintering, it is identical to sintering of pure iron powder. At medium oxide contents, an intermediate version is realized.

To determine the density of sponge iron after sintering compositions of various compositions, its calculation was carried out depending on the volume content of oxide and different dispersion of the iron powder. The compacts were made of pulverized iron powder of grade PjP2-200 with an average particle size of about 100 mkm and oxide (Fe_2O_3) with a particle size of 0.2-0.4 mkm by cold pressing. The calculation was carried out in the following sequence;

1. Volumetric composition of compacts:

$$V_{pr} = V_{i.p} + V_{ox} + V_{bin}$$

where, $V_{i.p}, V_{ox}\ and V_{bin}$ - respectively, the volume of iron powder, oxide and binder, sm^3.

$$V_{i.p} = \frac{m_{i.p}}{7.8},\ V_{ox} = \frac{m_{ox}}{5.24},\ V_{bin} = \frac{m_{bin}}{1.3}$$

where, $m_{i.p}, m_{ox}, m_{bin}$ are, respectively mass of iron powder, oxide and binder;

2. The volume of sintered billets was determined experimentally:

$$V_{sin} = V_{i.p} + \frac{V_{ox}\cdot 5.24\cdot 0.7}{7.8} + V_{pow}$$

The second term of the equation is the volume of iron, $(V_{zh.v})$, obtained as a result of oxide reduction.

V_{pow} is the volume of pores in the sintered compact.

$V_{pow}+V_{zh.v}$ is the volume of sponge iron obtained as a result of oxide reduction and subsequent sintering.

3. Density ($\rho_{s.g.}$) was calculated by the formula:

$$\rho_{s.g.}=\frac{m_{ox}\times 0.7}{V_{sin}-V_{i.p}}$$

The calculation results are shown in Table 4.

Table 4. Calculation results

No. Compositions	$\frac{Fe_1}{Fe_1+Fe_2}$	Density at temperatures, g/cm^3	
		1050 °C	1150 °C
1	1	3.28 (3.28)	4.13(4.13)
2	0.41	3.11 (4.68)	3.68 (5.07)
3	0.41	2.34 (4.06)	3.6 (4.68)

From Table 4, the addition of iron powder to the composition leads to a decrease in the density of the sponge iron. This decrease increases with increasing particle size of the iron powder. This contradicts the results shown in Figure 2. However, one should distinguish between an increase in the compacting density and an increase in the density of sponge iron. The addition of iron powder, on the one hand, reduces the density of the sponge iron, and on the other, increases the compacting density by increasing the volume content of the dense phase. A decrease in the density of sponge iron in the presence of iron particles of a lower dispersion in it can obviously be explained by the fact that they prevent shrinkage.

The fact of the presence of a low density of spongy iron, which does not correspond to the existing pores, draws on itself (Figure 3). This is apparent!} due to the fact that the sponge iron particles obtained by the reduction of a highly dispersed oxide have a high porosity, which is not detectable even at a magnification of 5000 times. Examination of the fine structure of reduced iron particles using an NTEGRA Prima microscope showed that the size of reduced iron is 100-300 nm (Figure 4). Particles up to l00 nm in size can be seen between these particles. The presence of such a structure, apparently, explains the low density of spongy iron sintered at a temperature of 1100 °C.

5. CONCLUSIONS

1) When determining the formulations of compositions based on "iron-oxide-binder" for complex shaped workpieces, as well as dispersed- perfect materials obtained by reaction grinding, one should take into account the double role of carbon in them.

2) When pressing the compositions to obtain shaped fillings of complex configuration, the content of carbon and resin (FFS) determines the rheological properties of the composition, inch its viscosity.

3) Analytical expressions have been obtained for formulations of compositions, which can be used by applying the appropriate correction factors.

4) Consolidation during sintering, depending on the composition of the compositions, has a complex character. With an increase in the proportion of oxide in the composition of the compositions from 0 to 11%, the relative density does not change. A further increase in the amount of oxide leads to a decrease in density. This regularity is manifested to a greater extent at low temperatures of isothermal holding (1050-1150 °S).

5) The introduction of iron powder into the composition of the compositions leads to a decrease in the density of the sponge iron. This decrease increases with an increase in the size of the iron powder particles

6) It has been established that during the reaction grinding of dispersed particles of iron oxide and pure iron powder using phenol-formaldehyde resin, leaching occurs, that is, carburization of the mixture. This circumstance can be used in the case of obtaining powder structural products with the highest rolling characteristics.

REFERENCES

[1] M. Randall, German, "Divergences in Global Powder Injection Molding", Powder Injection Molding International, Vol. 2. No. 1, pp. 45-49, 2008.

[2] M Randall German, "Designing for Metal Injection Molding: A Guide for Designers and End-users", Powder Injection Molding International, Vol. 2, No. 4, pp. 17-25. 2008.

[3] Ch. Schumacher, "New Options for Construction Design With the MIM-Process", Ceramic Forum International, Fraunhofer IIS Verlag, pp. 32-35, Stuttgart, Germany, October 2006.

[4] V.V. Skorohod, "Kinetic Equation for Densification, Grain Growth and Diffusion Alloying at Liquid-Phase Sintering of Multi-Component Systems", Proc., of PM-World Congress, Vol. 2, pp. 87-94, Vienna, Austria, October 17-21, 2004.

[5] R.N. Kadushnikov, V.V. Skorod, O.B. Lykova, "Computer Modeling of the Evolution of the Micro Structure of Two-Phase Polydisperse Materials During Sintering", Powder Metallurgy, No. 4, pp. 13-20, 1983.

[6] B.B. Skorokhod, "Structural Dynamics, Rheology and Macro Kinematics of Specfnium of Highly Dispersed Powders", In the Book, Properties and Application of Dispersed Powders, Vol. 4, No. 1, pp. 91-98, Naukova Dumka, Kiev, Ukraine, 1986.

[7] B.B. Shorokhod, "Rheological Properties of Carbonyl Iron", Nauk. Dumka, p. 150, Kiev, Ukraine, 1972.

[8] L.I. Tuchinsky, C.A. Zakharov, N.P.Pavlenko, "Sintering of Capillary-Porous Materials Based on Carbonyl Iron", Powder Metallurgy, No. 3, pp. 24-29, 1994.

[9] Ya.E. Geguzin, J.I.H. Paritskaya, "On the Interrelationships of Recrystallization and Homogenization Processes in Two-Component Mixtures of Ultrafine Powders", In the Book: Properties and Application of Dispersed Powders, Naukova Dumka, pp. 114-127, Kiev, Ukraine, 1986.

[10] G. Kuhling, "Handbook of Physics", M. Mir, p. 490, 1982.

[11] J.M. Contreras, A.J. Morales, J.M. Torralba, "Study of the Rheological Properties of a New Bronze 90 10 Feedstock Based on the Irregular Powder Particles for Application in Powder Injection Molding (PIM)", Powder Injection Molding Interna., Vol. l, No. 3, pp. 59-62, 2007.

[12] G. Kukla, G. Landgecker, W. Friesenbichler, "Duretek J. Flow Behavior of Feedstocks Proc. Of the PM", World Congress, Vienna, Austria, 17-21 October 2004.
[13] L. Nyborg, E. Zohansson, S. Niederlanser, "Assessment of Rheology and Related Proports of PIM - Feedstock Material", Proc., of Euro. PM., Feedstock Rebinding's, pp. 64-74, Norway, 2000.
[14] B.H. Antsiferov, V.D. Khramtsov, "Morphology of Powders and Rheology of Stabilized Suspensions", Proceedings of Universities, Powder Metallurgy and Functional Coatings, No. l, pp. 3-6, 2008.
[15] C. Hinse, R. Zauner, R. Nagel, P. Davies, M. Kearns, "Simulation Based Design for Powder Injection Molding", ZPowder Injection Molding International, Vol. 1, No. 2, pp. 54-56, 2007.
[16] J.L. Fan, Z.X. Li, B.Y. Huang, U.S. Cheng, T. Lin, "Debunking Process and Carbon Content Control of Hard Metal Components by Powder Injection Molding", Powder Injection Molding International, Vol. l, No. 2, pp. 57- 62, 2007.
[17] Z. Chi, X. Bo, W. Ziguoing, "Research of the Metal Injection Molding of Housings for the Semiconductor Industry", Powder Injection Molding International, Vol. 1, No. 4, pp. 56-59, 2007.
[18] C. Wu, V. Sunder, Arte, S. Laddha, Sh. Lee, K. Simmons, S.Z. Park, M. Randall German, D.T. Whuchell, "Material Homogeneity in Powder Injection Molded Ceramic Microchannel Arrays", Powder Injection Molding International, Vol. 2, No. 2, pp. 68-73, 2008.
[19] J.E. Bidaux, A. Jachem, E. Carreno Morelli, "Powder Injection Moldings of N_iT_i Shape Memory Materials", Powder Injection Molding International, Vol. 2, No. l, pp. 59-62, 2008.
[20] R.A. Iskanderov, J.M. Tabatabaei, "Vibrations of Fluid-Filled Inhomogeneous Cylindrical Shells Strengthened with lateral Ribs", International Journal on Technical and Physical Problems of Engineering (IJTPE), Issue 42, Vol. 12, No. 1, pp. 121-125, March, 2020.

BIOGRAPHIES

Name: **Chingiz**
Middle Name: **Arif**
Surname: **Aliyev**
Birthday: 07.07.1978
Birthplace: Baku, Azerbaijan
Bachelor: Hydraulic Machines, Hydraulic Couplings and Hydro Pneumo Automatics, Faculty of Petroleum Mechanics, Azerbaijan State University of Petroleum and Industry, Baku, Azerbaijan, 2000
Master: Hydraulic Machines, Hydraulic Couplings and Hydro Pneumo Automatics, Faculty of Petroleum Mechanics, Azerbaijan State University of Petroleum and Industry, Baku, Azerbaijan, 2002
Doctorate: Ph.D., Machines and Units of Oil and Gas Industry, Department of Machinery, Equipment and Processes, Azerbaijan State University of Petroleum and Industry, Baku, Azerbaijan, 2011
The Last Scientific Position: Assoc. Prof., Department of Mechanics, Faculty of Mechanical Engineering and Robotics, Azerbaijan Technical University, Baku, Azerbaijan, Since 2022
Research Interests: Hydraulics, Hydropneumatics Equipment
Scientific Publications: 115 Papers, 2 Monograph, 2 Patents

Name: **Jahangir**
Middle Name: **Vali**
Surname: **Asgarov**
Birthday: 09.08.1958
Birthplace: Fuzuli, Azerbaijan
Master: Faculty of Construction, Azerbaijan University of Architecture and Construction, Baku, Azerbaijan, 1980
Doctorate: Ph.D., Building Structures, Moscow Engineering and Construction Institute, Moscow, Russia, 1988
The Last Scientific Position: Assoc. Prof., Department of Reinforced Concrete Structures, Azerbaijan University of Architecture and Construction, Baku, Azerbaijan, Since 1996.
Scientific interests: Reinforced Concrete, Metal and Wooden Structures, Structural Mechanics
Scientific Publications: 60 Papers, 3 Textbooks

Name**:** **Aziza**
Middle Name**:** **Mursal**
Surname: **Guliyeva**
Birthday: 02.09.1960
Birthplace: Saatli, Azerbaijan
Master: Faculty of Construction, Azerbaijan University of Architecture and Construction, Baku, Azerbaijan, 1982
Doctorate: Ph.D., Building Structures, Azerbaijan University of Architecture and Construction, Baku, Azerbaijan, 1987
The Last Scientific Position: Assoc. Prof., Department of Reinforced Concrete Structures, Azerbaijan University of Architecture and Construction, Baku, Azerbaijan, Since 2000
Scientific Interests: Reinforced Concrete, Metal and Wooden Structures, Structural Mechanics. Scientific, Metal Science
Publications: 45 Papers, 3 Textbooks